Molecular and Cellular Pathobiology

Cancer Research

Cellular Disposal of miR23b by RAB27-Dependent Exosome Release Is Linked to Acquisition of Metastatic Properties

Marie Stampe Ostenfeld[1], Dennis K. Jeppesen[1], Jens R. Laurberg[1], Anders T. Boysen[2], Jesper B. Bramsen[1], Bjarke Primdal-Bengtson[1], An Hendrix[3], Philippe Lamy[1], Frederik Dagnaes-Hansen[4], Mads H. Rasmussen[1], Khan H. Bui[5], Niels Fristrup[1], Erik I. Christensen[6], Iver Nordentoft[1], Jens P. Morth[7], Jørgen B. Jensen[8], Jakob S. Pedersen[1], Martin Beck[5], Dan Theodorescu[9], Michael Borre[8], Kenneth A. Howard[2], Lars Dyrskjøt[1], and Torben Falck Ørntoft[1]

Abstract

Exosomes are small secreted vesicles that can transfer their content to recipient cells. In cancer, exosome secretion has been implicated in tumor growth and metastatic spread. In this study, we explored the possibility that exosomal pathways might discard tumor-suppressor miRNA that restricts metastatic progression. Secreted miRNA characterized from isogenic bladder carcinoma cell lines with differing metastatic potential were uncoupled from binding to target transcripts or the AGO2–miRISC complex. In metastatic cells, we observed a relative increase in secretion of miRNA with tumor-suppressor functions, including miR23b, miR224, and miR921. Ectopic expression of miR23b inhibited invasion, anoikis, angiogenesis, and pulmonary metastasis. Silencing of the exocytotic RAB family members RAB27A or RAB27B halted miR23b and miR921 secretion and reduced cellular invasion. Clinically, elevated levels of RAB27B expression were linked to poor prognosis in two independent cohorts of patients with bladder cancer. Moreover, highly exocytosed miRNA from metastatic cells, such as miR23b, were reduced in lymph node metastases compared with patient-matched primary tumors and were correlated with increments in miRNA-targeted RNA. Taken together, our results suggested that exosome-mediated secretion of tumor-suppressor miRNA is selected during tumor progression as a mechanism to coordinate activation of a metastatic cascade. *Cancer Res; 74(20); 5758–71. ©2014 AACR.*

Introduction

Bladder cancer is the fifth most common malignancy among men. Approximately 75% of patients with bladder cancer have frequently recurring non–muscle-invasive tumors (Ta, T1, or CIS). The remaining 25% of patients are diagnosed with muscle-invasive cancer (T2–T4) with eventual metastatic spread to lymph nodes, bones, liver, and lungs. The mechanism of metastasis is largely unknown and patients are, therefore, treated with nontargeted combination chemotherapy. However, only half of the patients respond, leading to poor patient survival (1). There is, therefore, an urgent need for improved understanding of the mechanisms leading to metastatic bladder cancer.

Carcinoma cells acquire distinct properties during metastatic colonization. These include migration and invasion in the primary tumor setting, intravasation and extravasation of the bloodstream, resistance to anoikis when in circulation, and finally outgrowth from micrometastases in distant organs. To address molecular events of metastatic bladder cancer, isogenic human bladder carcinoma cell lines with different metastatic capacity have previously been established through iterative injections of parental cell lines into mice (2, 3). A metastasis expression signature was deduced and specific genes were identified that suppress (RhoGDI2/ARHGDIB) or stimulate (LAMC2 and sialoglycoprotein CD24) metastatic progression (2–4). Tumor exosomes have been implicated in promoting metastatic spread of breast cancer and melanoma in mouse models (5–7). We, therefore, speculated if the release of exosomes and their specific content contribute to the metastatic behavior of the isogenic bladder cancer cells.

Exosomes are small vesicles (30–100 nm) that are secreted by various cells. They originate from inward budding into multivesicular bodies (MVB; ref. 8). Upon MVB fusion with the plasma membrane, the intraluminal vesicles are released into the extracellular space as exosomes, a process regulated, for e.g., by small GTPases RAB27A/B, as well as SMPD3/

[1]Department of Molecular Medicine (MOMA), Aarhus University Hospital, Skejby, Denmark. [2]The interdisciplinary Nanoscience Center (iNANO), Aarhus University, Denmark. [3]Laboratory of Experimental Cancer Research, Ghent University Hospital, Belgium. [4]Department of Biomedicine, Aarhus University, Denmark. [5]EMBL Heidelberg, Heidelberg, Germany. [6]Department of Biomedicine–Anatomy, University of Aarhus, Denmark. [7]Centre for Molecular Medicine Norway (NCMM), University of Oslo, Norway. [8]Department of Urology, Aarhus University Hospital, Denmark. [9]University of Colorado Cancer Center, Aurora, Colorado, USA.

Note: Supplementary data for this article are available at Cancer Research Online (http://cancerres.aacrjournals.org/).

L. Dyrskjøt and T.F. Ørntoft contributed equally to this article.

Corresponding Authors: Marie Stampe Ostenfeld and Torben Falck Ørntoft, Department of Molecular Medicine (MOMA), Aarhus University Hospital Skejby, Brendstrupgaardsvej 100, DK-8200 Aarhus N, Denmark. Phone: 45-8949-9400; Fax: 45-8678-2108; E-mail: marie.stampe@clin.au.dk and orntoft@clin.au.dk

doi: 10.1158/0008-5472.CAN-13-3512

NSMASE2 (9–11). The vesicles were first discovered in differentiation of reticulocytes, during which obsolete transferrin receptors (TFR) were removed by exosome release (12). Exosome pathways may also facilitate the exocytosis of key molecules in cancer. Exosomal tetraspanins CD82 and CD9 restrain intracellular WNT signaling by targeting β-catenin/CTNNB1 for exosome release (13); viral LMP1 (encoded by Epstein–Barr virus) is secreted in CD63-exosomes as an antagonizing mechanism for LMP-1–mediated constitutive NF-κB activation (14), and active tumor-suppressor PTEN is exocytosed and transferred to other cells via exosomes (15). These studies highlight a possible cellular disposal role by exosomes. On the other hand, exosomes can transfer functional miRNAs to recipient cells (16, 17) and tumor exosomes may promote oncogenic signaling in recipient cells upon delivery of cargo (7, 18).

miRNAs are approximately 21 nt regulatory molecules that repress mRNA target translation. They are transcribed as long primary transcripts, processed into hairpin precursors by DROSHA, cleaved by DICER into mature miRNAs that then may bind argonaute (AGO) proteins for loading into the miRNA-induced silencing complex (miRISC). Exosomes contain precursor- and mature miRNAs at altered relative abundance compared with their cellular expression (17, 19), and modulate gene expression in recipient cells (10, 17). The vesiculation of miRNAs may depend on sequence motifs and protein sumoylation (20, 21). miRNAs with tumor-suppressor function are often lost in cancer (22). In this study, we analyzed whether the release of exosomes and their specific miRNA cargo were coupled to a metastatic behavior of bladder carcinoma cells and if miRNA exocytosis could be of intrinsic advantage to cancer cells themselves. Our results demonstrate that exocytosed miRNAs are decoupled from mRNA target and miRISC association. Moreover, miRNA secretion can be inhibited by RAB27A and -B knockdown that consequently lead to the intracellular upregulation of functionally active miR23b. This miRNA suppressed various steps of the metastatic process (invasion, angiogenesis, anoikis resistance, and lung colonization). Data from clinical samples linked RAB27B with poor prognosis of bladder cancer patients and loss of miR23b during lymph node colonization of tumor cells. In conclusion, our data suggest that exosome release may be a route to cellular disposal of tumor-suppressor miRNAs with intrinsic advantages to the parental cell.

Materials and Methods

Clinical samples, cell culture, and reagents

All patients gave written consent, and the study was approved by the Central Denmark Region Committees on Biomedical Research Ethics (1994/2920 and 20040110). Primary tumors and patient-matched lymph node metastases were laser microdissected (>90% carcinoma cells) using the PALM laser microbeam system. Human primary urothelial cells (obtained from Prof. J. Catto, Department of Oncology, University of Sheffield, United Kingdom) and transitional carcinoma cells T24 (purchased from ATCC in 2009), SLT4, FL3, UMUC3, and LUL2 (obtained from Prof. Dan Theodorescu, University of Colorado Cancer Center, Aurora, CO, in 2010) were used in the study. Cell line authentification was conducted by Promega Cell-ID kit (IdentiCell, MOMA; Supplementary Fig. S1C). Last testing was conducted in January 2014. Metastatic SLT4 and FL3 cell lines are isogenic derivatives of the poorly metastatic T24T and its nonmetastatic parental cell line T24. SLT4 metastasizes primarily to the liver (2). FL3 and LUL2 have been generated from tail vein injections using T24T and UMUC3 cells, respectively, with resultant lung metastases (2, 3).

In vivo experiments and ddPCR

Neovascularization was examined by CAM assay. NCr nude mice (Taconic) were tail-vein injected with 1×10^6 cells. At 4/6 weeks, mice were killed (4 at each time point), lungs were harvested, and processed for immunohistochemical staining or ddPCR. Three human-specific DNA sequences at chromosome 3, 7, and 12 were quantified by ddPCR using QX100 Droplet Digital system (Bio-Rad Laboratories Inc.).

Exosome isolation

Cells were propagated in 3×150 cm^2 flasks or CELLine Adhere1000 bioreactors (Integra Biosciences) for exosome isolation. Cells were propagated in DMEM supplemented with 10% FCS until 90% confluency, washed three times in PBS and replenished with advanced DMEM (Invitrogen) devoid of FCS or in DMEM + 10% exosome-depleted FCS (by 100,000 × *g* overnight centrifugation). The media were harvested and samples were processed when viability exceeded 95% (Trypan blue exclusion, Cedex XS; Roche Innovatis AG). Bioreactor cultivation was conducted as previously described (23).

Culture media were subjected to differential centrifugation of 3,200 × *g* (10 minutes) to remove residual cells and cellular debris, 16,000 × *g* (30 minutes) to remove apoptotic bodies and microparticles, and 100,000 × *g* (2 hours) to pellet exosomes (rotors: Type 70 Ti and Sorvall surespin 630 used in ultracentrifuges Beckman coulter and Sorvall Discovery 100SE by Hitachi, respectively). Exosome pellets were washed in PBS and centrifuged at 100,000 × *g*. Pelleted exosomes were added to 1,100 μL Qiazol for RNA extraction, PBS for nanoparticle tracking analysis (NTA), and SDS sample buffer for immunoblotting.

Nanoparticle tracking analysis

Vesicle size/concentration was analyzed by NanoSight LM10 system and NTA software v2.3 (NanoSight Ltd), calibrated at 183 nm/pixel using 100-nm calibration beads. Video recordings of 60 to 90 seconds and approximately 500 to 1,500 tracks were analyzed per sample.

Protein detection

Quantification of secreted protein was performed using the MicroBCA assay (Thermo Fischer). Immunoblotting of cellular and exosomal protein content was conducted using antibodies against RAB27A (Abcam; ab55667), RAB27B (Immuno-Biological Laboratories; 18973), Alix (Cell Signaling Technology; clone 3A9), CD63 (Pharmingen BD), Hsp90, CD81, and Tsg101 (Santa Cruz Biotechnology), and VDAC and β-actin (Abcam).

Cell viability, real-time invasion monitoring, and anoikis assay

Trypan blue exclusion followed by automatic cell counting and MTT (Sigma-Aldrich) reduction assay was used to

measure the cell viability, essentially as described (24). Cellular morphology and plasma membrane integrity was monitored by phase-contrast microscopy using a Zeiss Axiovert 40 CFL microscope.

Real-time invasion assays were conducted on CIM-16 plates using xCELLigence System (Roche). Invasion was quantified by calculation of the slope increment of a period of time (T0–T9 hours or T0–T20 hours) using RTCA software. Resistance to anoikis was quantified by plating 1.6×10^5 cells on Corning costar ultra-low attachment 24-well plates (Corning Life Sciences).

miRNA and mRNA quantification

RNA was extracted using the miRNeasy Mini Kit (Qiagen Sciences) by inclusion of MS2 carrier RNA (Roche) and cel-miR39 spike-in (DNA Technology A/S) for technical validation. RNA integrity was assessed using a 2100 Bioanalyzer (Agilent Technologies). miRNA expression profiling of exosomes and parental cells was performed using the stem loop RT-qPCR based TaqMan Low Density Array Human MicroRNA A+B cards (Applied Biosystems) v2.0 for exosomes/cultivated cells and v3.0 for primary tumors versus metastases, essentially as described (25). mRNA profiling was conducted using GeneChip Human Gene 1.0ST, 2.0ST, and U133+ Arrays (Affymetrix).

AGO2 immunoprecipitation

Scr- and RAB27B siRNA-transfected cells were scraped off culture flasks in gentle lysis buffer, processed, and incubated with AGO2 antibody (11A9; Sigma-Aldrich)-bound Protein G–coupled Magnetic Dynabeads (Life technologies), or anti-FLAG as a negative control (F1804; Sigma-Aldrich). Total RNA from input, AGO2-IP, and FLAG-IP were purified and miR23b and selected mRNAs were subsequently quantified by RT-qPCR TaqMan assays.

Statistical analysis

Statistical testing was conducted by linear regression, parametric (t test), or nonparametric (Wilcoxon–Mann–Whitney, Kolmogorov–Smirnov) testing when appropriate. $P < 0.05$ was considered significant. miRNA target site

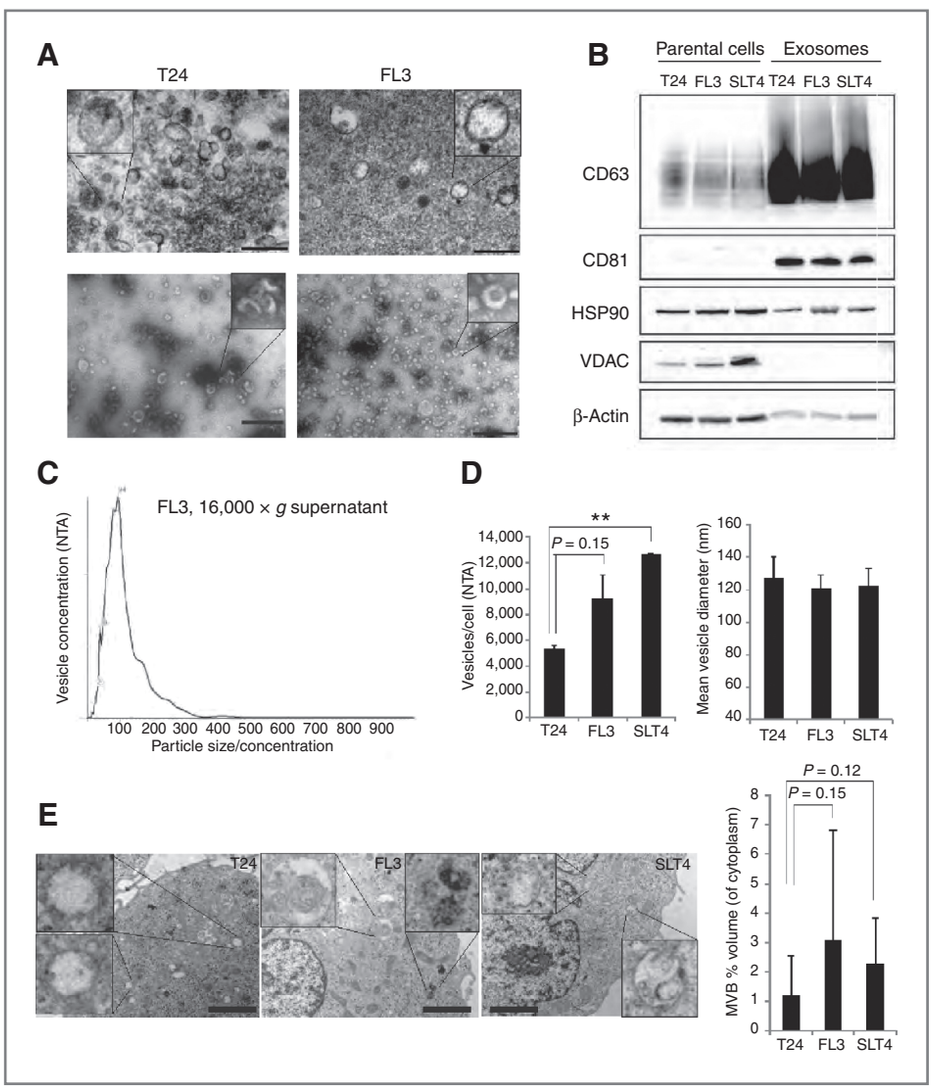

Figure 1. A, top, electron microscopy analysis of epon-embedded exosomes; scale bar, 200 nm. Bottom, negative stain electron microscopy of exosomes; scale bar, 500 nm. B, immunoblotting for exosomal markers CD63, CD81, as well as HSP90, VDAC, and β-actin/ACTB. C, size distribution of FL3-secreted vesicles as analyzed by NTA. D, number of vesicles released per cell (left) and the mean modal vesicle size (nm; right). E, left, electron microscopy of cells; scale bar, 2 μm, close-up of representative MVBs. Right, quantification of the number of MVBs (% volume of the cytoplasm). Columns in D, averages of triplicate measurements of three experiments; bars, SD; **, $P < 0.01$ compared with T24. Columns in E, averages of $n = 10$ cells.

analysis was conducted using TargetScanS, Gene Set Enrichment Analysis (GSEA), and UCSC genome browser.

(Additional details are provided in Supplementary Information).

Results

Isolation, characterization, and secretion of exosomes from urothelial carcinoma cell lines with different metastatic properties

To investigate possible differences in exocytosis of miRNAs related to metastatic propensity, exosomes were isolated from isogenic bladder carcinoma cells with different metastatic capacity in mice by differential centrifugation. Electron microscopy of T24 and FL3-secreted vesicles revealed round-shaped double-lipid membrane vesicles upon epon-embedment, whereas cup-shaped upon negative stain (Fig. 1A). Immunoblotting demonstrated vesicular enrichment of tetraspanins CD63 and CD81, and presence of HSP90, ALIX, TSG101, and β-actin (Fig. 1B and Supplementary Fig. S1A). Minimal presence of contaminating mitochondrial VDAC was observed.

The size and concentration of vesicles was examined by NTA. The profiles were more homogenous from 16,000 × *g*

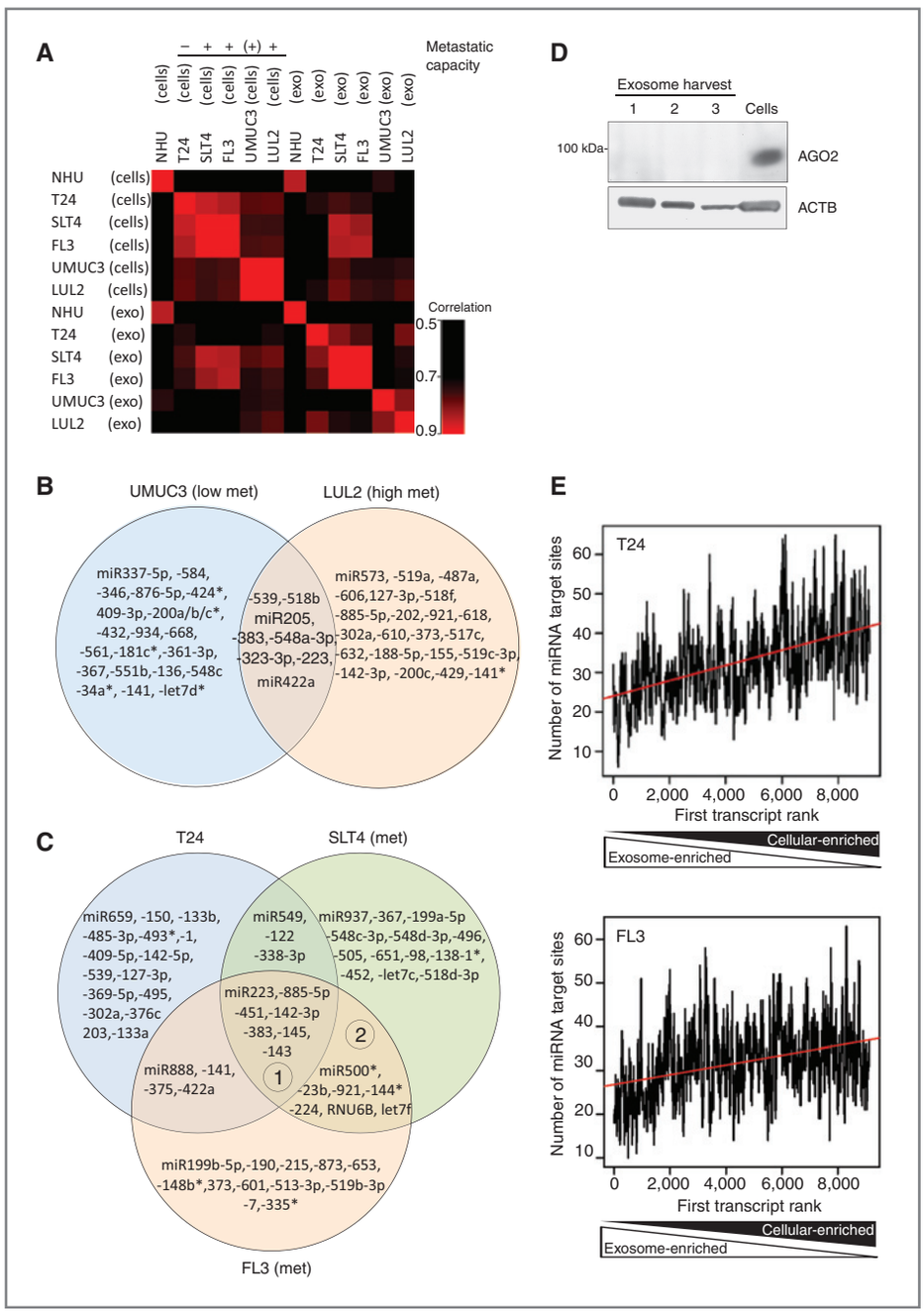

Figure 2. A, Pearson correlation coefficient-based heatmap representation of the similarity of miRNA expression profiles from cells and their released exosomes (high correlation, intense red). B and C, Venn diagrams depicting the top 30 exosome-secreted miRNAs. D, immunoblotting of AGO2 and ACTB from T24 cells and three independent exosome harvests. E, the number of miRNA targets (for the top 30 exocytosed miRNAs) present in cellular and exosomal transcripts (red line, linear regression).

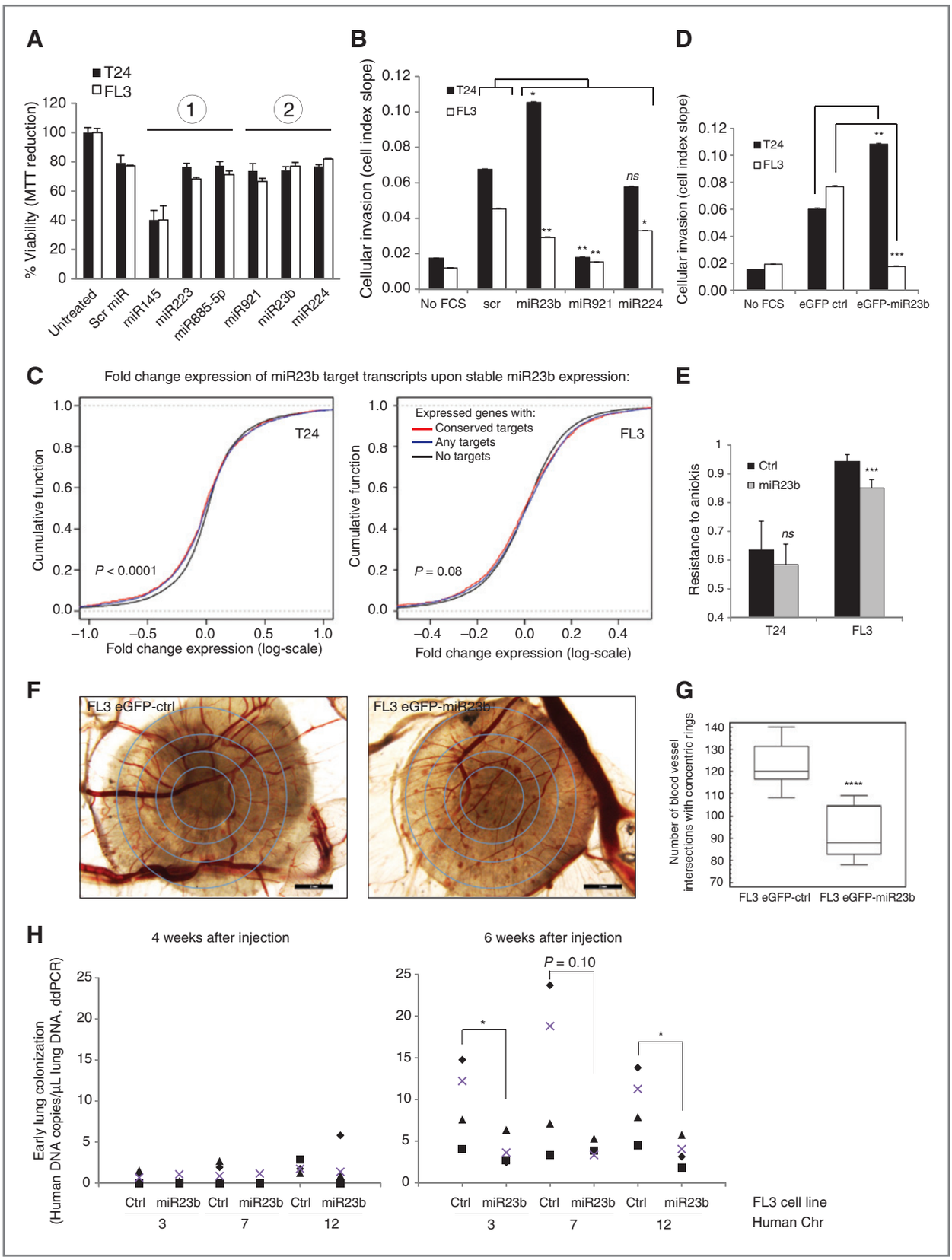

supernatants than from 100,000 × *g* pellets, likely due to vesicle aggregates upon 100,000 × *g* sedimentation (Fig. 1C and Supplementary Fig. S1B). Subsequent quantitation was, therefore, performed on 16,000 × *g* supernatants. Increased number of secreted vesicles was observed for the metastatic cell line SLT4 ($P < 0.01$), but not significantly for FL3 ($P = 0.15$) in comparison with their nonmetastatic isogenic parental cell line T24 (Fig. 1D, left). The mean vesicle size (~120 nm) was equivalent (Fig. 1D, right). MVBs are sites of exosome biogenesis and we, therefore, analyzed for possible differences in MVB volume percentage. Small vesicles included in MVBs were observed and a slight increase in MVB volume density in FL3 and SLT4 cells, although not significant (Fig. 1E), was also observed. Overall, the results indicated elevated, but not profound, exosome release from metastatic versus nonmetastatic cells.

Characterization of miRNA exocytosis from primary urothelial cells and bladder carcinoma cells

We next profiled the expression of 667 unique human miRNAs in cells and their exosomes released over 24 hours by RT-qPCR. In addition to T24, SLT4, and FL3, isogenic bladder carcinoma UMUC3 (low-metastatic) and LUL2 (high-metastatic) cells, and primary human urothelial cells were included. The miRNA expression was significantly altered in carcinoma versus primary cells and exosomes, and correlated more between FL3 and SLT4 exosomes (from metastatic cells) than between T24 (nonmetastatic) and FL3/SLT4 exosomes (Fig. 2A; Supplementary Fig. S1D; Supplementary Table S1).

Next, cell-to-vesicle miRNA abundances were compared by nonparametric ranking analysis. A delta-rank score (vesicles versus cells) was calculated to identify relative highly exocytosed miRNAs (Fig. 2B and C, Supplementary Fig. S1E). Interestingly, some miRNAs were exclusively observed in vesicles and not in the parental cells (e.g., miR921), and some miRNAs were exclusively retained in cells (e.g., miR330-5p; Supplementary Table S2).

We analyzed whether the export of miRNAs was coupled to binding of miRISC complex proteins and putative target transcripts. First, from our recent quantitative proteomic study on exosomes (23), we observed no spectral counts for miRNA processing proteins (DICER and DROSHA) or miRISC-associated proteins (TNRC6A/GW182 and TARBP2P/TRBP; Supplementary Table S3A). AGO1 and AGO2 were detected in one of three replicates. However, immunoblotting revealed no detectable AGO2 (Fig. 2D). Second, mRNA profiling was conducted on cells and exosomes. The vesicles were deprived in transcripts containing target sites for the top 30 highly exported miRNAs (Fig. 2E). Instead, a significant higher number of target sites was detected in the cellular-enriched pool of transcripts ($P < 2E10^{-16}$ for all six cell types; Fig. 2E and Supplementary Fig. S1F). Together, the results suggest that exocytosed miRNAs are not engaged in miRISC activity, and that exocytosis of specific miRNAs is coupled to high intracellular levels of their putative target transcripts.

We noticed that miR143 and -145 were relatively highly secreted from T24, FL3, and SLT4 cells (Fig. 2C). We previously identified these as tumor suppressors in bladder cancer (26, 27). Exosome-mediated transfer of miR143 inhibits proliferation of recipient cells (28) and we speculated if exosomal pathways could be a means of miRNA tumor-suppressor elimination by the producing cell. Two groups of miRNAs were selected for further analysis (Supplementary Table S3B) based on (i) their exclusive exocytosis from carcinoma versus normal cells and/or (ii) their high relative secretion from metastatic versus nonmetastatic cells.

Tumor-suppressor function of selected exocytosed miRNAs from bladder carcinoma cells

Ectopic expression of miR145, miR223, miR885-5p (group 1) and miR23b, miR921, miR224 (group 2) was conducted by miRNA mimic transfection in T24 and FL3 cells (these cell lines were chosen as two extremes with respect to metastatic capacity). As expected, miR145 markedly reduced cell viability, whereas the remaining miRNAs did not (Fig. 3A and Supplementary Fig. S2A). We then focused on relative highly secreted miRNAs from metastatic cells (group 2). Tissue dissemination is a crucial initial step during the metastatic process. We, therefore, examined the capacity of cells to invade Matrigel upon miRNA overexpression by xCELLigence. Cellular invasion was inhibited by miR23b, miR224, and miR921 in FL3 cells (Fig. 3B, Supplementary Fig. S2B–S2D), the latter of which was diminished by LNA-miR921 knockdown (Supplementary Fig. S2C). Similar effects were observed in (low)-metastatic UMUC3 cells (Supplementary Fig. S2F). On the contrary, cellular invasion was stimulated by miR23b and inhibited by LNA knockdown (Fig. 3B, Supplementary Fig. S2E) in nonmetastatic T24 cells.

To further investigate this, we cloned miR23b and miR921 into pEGFP-C1 vectors. Stable cell lines expressing miR921 could unfortunately not be expanded, but T24 and FL3 cells with 10 to 20-fold elevated miR23b expression were obtained (Supplementary Fig. S2G). mRNA profiling revealed enrichment of miR23b seeds and/or predicted targets among downregulated transcripts (Fig. 3C). The overall transcriptional changes in T24 and FL3 cells were, however, predominantly opposite with respect to up- and downregulation (Supplementary Fig. S2H). Consistent with transient expression, cellular invasion was reduced for FL3 cells and increased for T24 cells upon stable eGFP-miR23b expression

Figure 3. A, cells were transfected with the indicated miRNAs (10 nmol/L) and viability assessed by MTT reduction assay 48 hours after transfection. B, transfected cells were examined for their invasion capacity by real-time xCELLigence. C, stable cells expressing eGFP-ctrl and eGFP-miR23b were generated. Affymetrix Genechip analysis was conducted and the expression of predicted miR23b targets (targetScan; red) and mRNAs ± ≥one miR23b 7mer site in the 3′-UTR (blue and black, respectively) was examined. D and E, cellular invasion and anoikis resistance of stable cell lines. F and G, *in vivo* angiogenesis by CAM assay. Blood vessel formation was quantified 14 days after implantation of FL3 eGFP-ctrl ($n = 18$) and eGFP-miR23b ($n = 15$) cells. H, *in vivo* lung colonization. Lungs were excised 4 or 6 weeks after injection of cells into mice and examined by ddPCR targeting human-specific DNA (chromosome 3/7/12). Columns in A, B, D, E, averages of triplicate measurements; bars, SD. Data are representative of a minimum of three experiments (A, B, and D) or average of three experiments (E). Points in H, human DNA copies per μL mouse lung DNA. *, $P < 0.05$; **, $P < 0.01$; ***, $P < 0.001$; ****, $P < 0.0001$.

(Fig. 3D and Supplementary Fig. S2I). During the metastatic cascade, cancer cells avoid anoikis when arrested in circulation. In line with this, metastatic FL3 cells were more resistant to anoikis than nonmetastatic T24 cells (Fig. 3E). The anoikis resistance of FL3 cells was attenuated by stable expression of miR23b as previously documented for this miRNA (29).

We next addressed if miR23b acted as a tumor suppressor *in vivo*. miR23b significantly reduced angiogenesis in a CAM assay (Fig. 3F and G). When injected into the tail vein of mice, FL3 cells form lung metastases, whereas T24 cells do not (30, 31). Early lung colonization can be detected by a molecular PCR assay after 5 weeks, which correlates with subsequent macroscopic lung metastatic disease and Kaplan–Meier survival curves of mice (30). We examined early lung colonization in NCr nude mice upon tail vein injection of FL3 eGFP-ctrl and eGFP-miR23b cells. After 4 weeks, ddPCR of three human-specific DNA regions detected little or no human DNA (from FL3 cells) in mouse lungs. At 6 weeks, lung colonization was evident and a reduced tumor cell burden was observed upon injection of FL3 eGFP-miR23b versus eGFP-ctrl cells (Fig. 3H). Together, the results indicate that miR23b acts as a tumor suppressor at different steps of the metastatic process [invasion (in FL3), anoikis, angiogenesis, and lung colonization].

RAB27A/B in bladder cancer disease course and cellular invasion

We wished to investigate intrinsic functional consequences of blocking miRNA tumor-suppressor exocytosis. For this, we aimed to establish a model system of diminished exosome release. This has previously been accomplished by knockdown of RAB27A and -B GTPases, or by pharmacologic inhibition (GW4869) or knockdown of NSMASE2/SMPD3 (9, 10, 32).

Exome sequencing identified none or only one missense mutation in RAB27A and RAB27B, respectively (Supplementary Fig. S3A; ref. 33). Immunohistochemical staining of tumor cores revealed RAB27A staining in less than 1 of 40 biopsies. For RAB27B, a diffuse cytoplasmic staining of varying degree was observed in the carcinoma cells (Supplementary Fig. S4B). High RAB27B expression correlated to progression from non–muscle-invasive to muscle-invasive disease (Fig. 4A; $P = 0.011$, log-rank test), and with reduced cancer-specific survival among patients with advanced disease (Fig. 4B; $P = 0.046$, Supplementary Fig. S3B).

All the examined cell lines showed detectable RAB27A, RAB27B, and SMPD3 (Fig. 4C, Supplementary Fig. S3C). The steady-state level of RAB27A or -B did not correlate directly with the metastatic behavior of the cells. Previously, a 20-fold reduction in RAB27B expression upon cultivation of urothelial cells has been reported (34). Thus, direct comparisons of expression levels in clinical samples and cell lines may be difficult. Specific knockdown of RAB27A and -B was obtained (Fig. 4D and Supplementary Fig. S3D), whereas knockdown of SMPD3 was inconsistent and excluded from further analysis. RAB27B knockdown was accompanied by several transcriptional changes (Supplementary Table S3C; Fig. 4E).

The phenotypic consequence of RAB27A or RAB27B knockdown was subsequently examined. Cell morphology and viability was unaffected 72 hours after transfection (with exception of one RAB27A siRNA in FL3 cells; Fig. 4F; Supplementary Fig. S3E) and at later time points (Supplementary Fig. S3F). RAB27A or -B knockdown did, however, attenuate cellular invasion (Fig. 4G and Supplementary Figs. S3G and S4A). Combined knockdown showed no additive effects (Supplementary Fig. S4B). Overexpression of RAB27B increased migration and invasion of UMUC3 cells (Supplementary Fig. S4C). Finally, GW4869 pretreatment also inhibited cellular invasion (Supplementary Fig. S4D–S4F). The data indicate that RAB27A, RAB27B, and NSMASE2 are involved in regulation of cellular invasion, and that RAB27B is associated with poor prognosis of bladder cancer.

RAB27A and RAB27B knockdown reduces vesicle secretion and exocytosis of miR23b and miR921

We next established a model system to attenuate exosomal miRNA secretion. RAB27A and RAB27B knockdown reduced the number of vesicles present in 16,000 $\times$ *g* cell culture supernatant as detected by NTA (Fig. 5A), whereas GW4869 failed to inhibit secretion from FL3 cells (Fig. 5B). Knockdown also reduced the 100,000 $\times$ *g* pelleted vesicle fraction as measured by protein amount (Fig. 5C).

We then quantified the levels of exocytosed miRNAs. Knockdown of RAB27A and RAB27B decreased the exocytosis of miR23b and miR921. The effect of attenuation was similar and not additive upon combined knockdown (Fig. 5D). Treatment with GW4869 did not attenuate the release in accordance with no inhibitory effects on vesicle secretion (Fig. 5B and D). Exosomes are mainly pelleted at 100,000 $\times$ *g*. Accordingly, approximately 70% and 95% of the miR23b and miR921 signals were cleared upon 100,000 $\times$ *g* ultracentrifugation (Fig. 5E, Scr).

Attenuated miR23b exocytosis leads to increased miR23b activity in the parental cell

We next investigated intrinsic effects of attenuated miRNA exocytosis. Target transcript cleavage in miRISC relies on miRNA and target site abundances, sequence accessibility, and negative- and positive regulator expression (35, 36). We found that cellular transcripts most differentially regulated between FL3 and T24 also contained the largest number of (conserved) miRNA target sites (Supplementary Fig. S4G; $P < 0.01$). RAB27A and RAB27B knockdown was accompanied by an intracellular rise of (mature) miR23b, but not of pri-miR23b, in FL3 cells (Fig. 6A). We also analyzed T24 cells that secrete miR23b RAB27A/B-dependently but at a reduced relative rate (Figs. 2C and 5D). An intracellular rise in exact miR23b copies was observed upon RAB27B knockdown, which was not the case for cellular-retained miR330-5p (Fig. 6B).

Intracellular accumulation of miRNAs destined for exocytosis can either be functionally inactive due to encapsulation in intraluminal vesicles of MVBs or may accumulate in the cytosol to actively bind AGO2/miRISC proteins and direct target transcript degradation. To address this, we performed AGO2 immunoprecipitation experiments (Fig. 6C). RAB27B knockdown

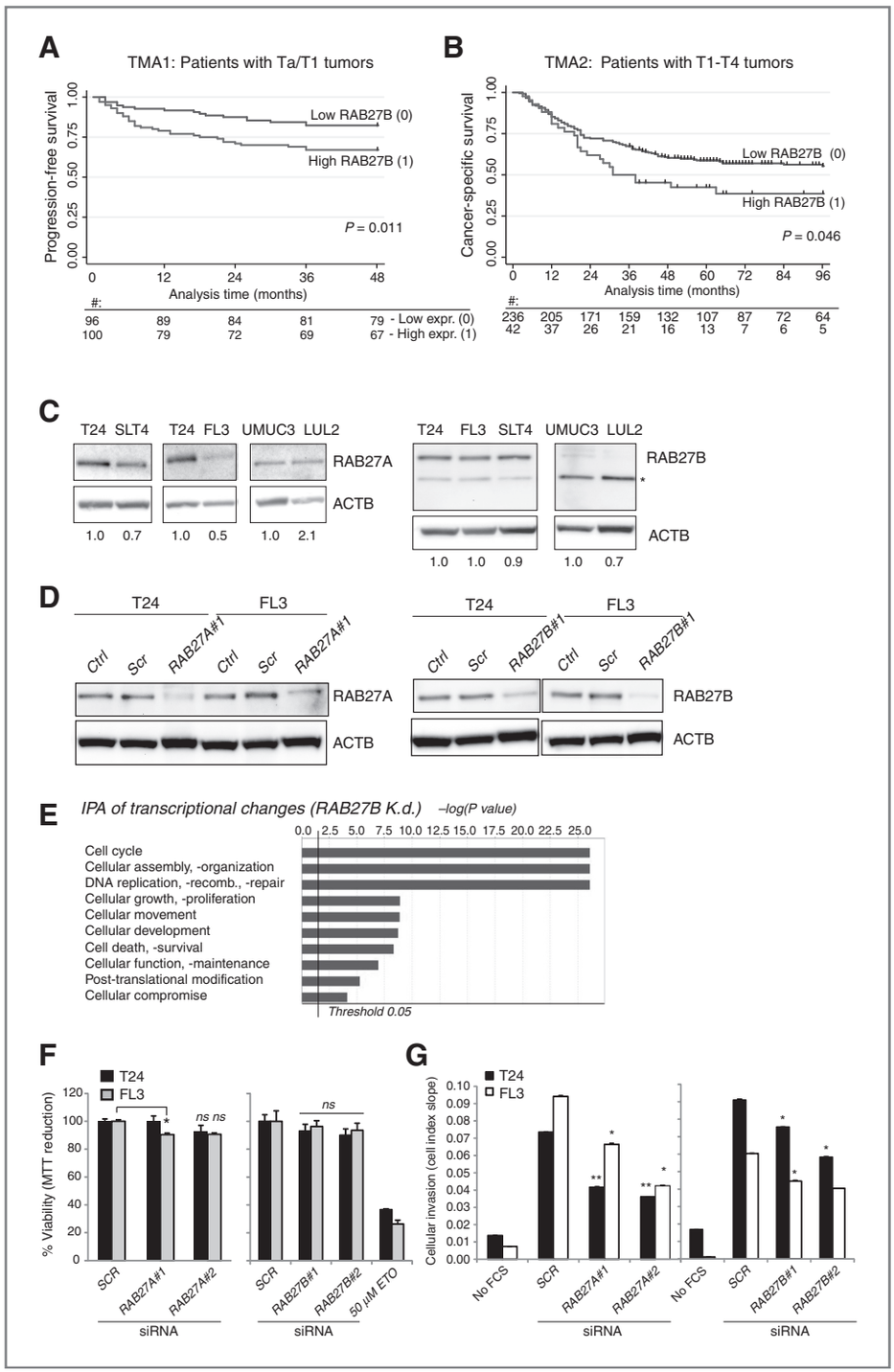

Figure 4. A and B, Kaplan–Meier plots of the risk of disease progression (A) and the cancer-specific survival (B) of patients as functions of RAB27B expression (*P* value, log-rank test). C, expression of RAB27B and RAB27A in the indicated cell lines as determined by immunoblotting. *, a shorter variant of RAB27B. D, knockdown of RAB27A and RAB27B 72 hours after transfection (20 nmol/L siRNA). E, Ingenuity Pathway Analysis of transcriptional changes upon RAB27B knockdown. F and G, cellular viability (F) and invasion (G, xCELLigence) analyzed 48 hours after transfection. Columns in F and G, averages, triplicate measurements; bars, SD; data are representative of two to four experiments; *, $P < 0.05$; **, $P < 0.01$.

resulted in elevated miR23b association with AGO2 (with varying degree in three experiments; Fig. 6D). The increase was accompanied by general elevated levels of four putative target transcripts (Fig. 6E), whereas ubiquitin was unchanged (Supplementary Fig. S4H).

On the basis of the observations that (i) RAB27B knockdown and miR23b overexpression inhibited cellular invasion of FL3 cells (Fig. 3B and D and 4H) and (ii) RAB27B knockdown increased intracellular functional miR23b, we finally tested if miR23b knockdown could rescue the diminished invasion observed by RAB27B knockdown. An LNA molecule against miR23b had no effect in itself (Supplementary Fig. S2E), however, reverted the attenuated invasion induced upon RAB27B knockdown (Fig. 6F). Together, the results indicated

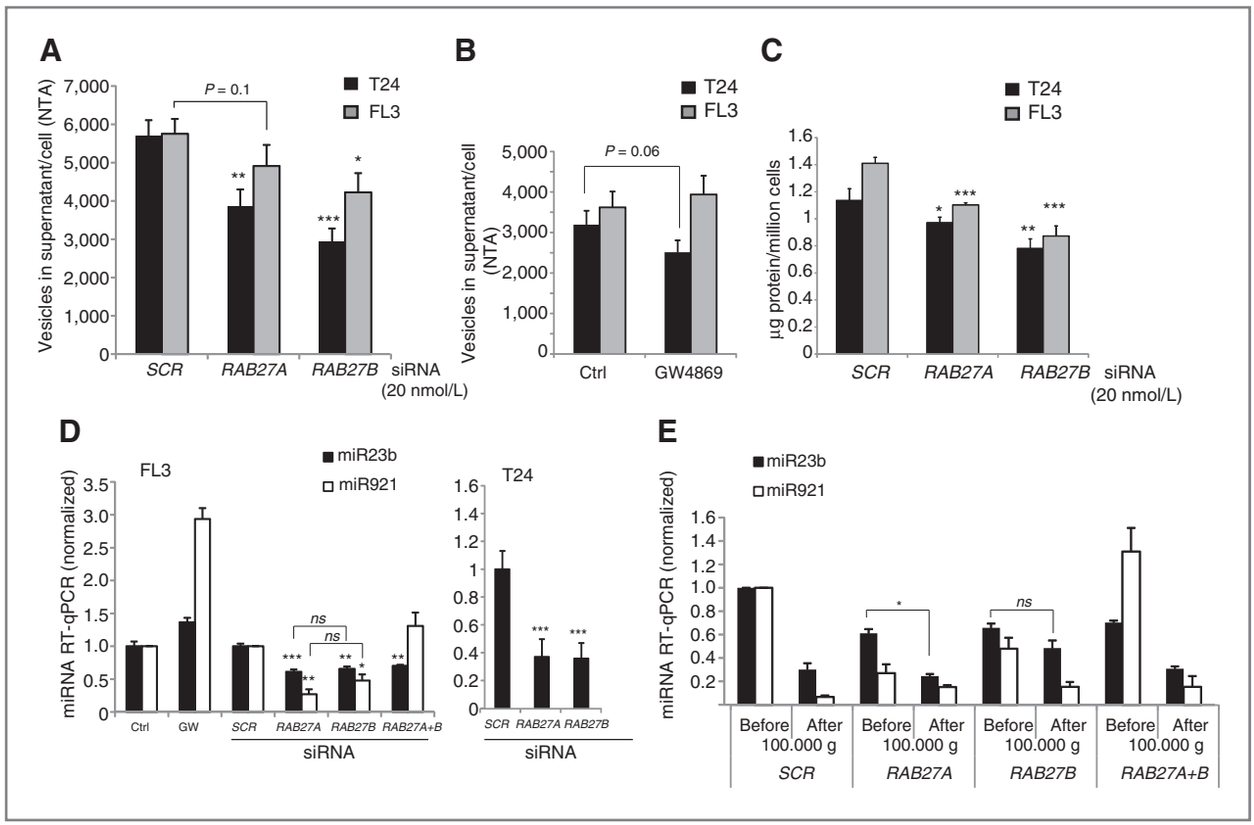

Figure 5. A and B, number of exosomes present in the 16,000 × *g* media supernatant 72 hours after siRNA transfection (A) or upon 48 hours treatment with GW4869 (B). C, protein amount in the 100,000 × *g* pellet after knockdown. D and E, quantification of exocytosed miR23b and miR921. D, quantity of miR23b and miR921 in the 16,000 × *g* supernatant. Cells were left untreated, treated with GW4869 (GW), or transfected with siRNAs. E, comparison of miRNA levels in the 16,000 × *g* supernatant versus supernatant obtained from subsequent 100,000 × *g*. Columns in A–C, averages of triplicate measurements; bars, SD. Data are representative of three experiments. Columns in D and E, averages of two independent experiments, each measured in three to six replicates; bars, SD. *ns*, not significant; *, $P < 0.05$; **, $P < 0.01$; ***, $P < 0.001$.

that attenuated exocytosis of miR23b was associated with intracellular accumulation and increased functional activity.

miRNA expression analysis in clinical samples of metastatic bladder cancer

The expression of the group 1 and 2 exocytosis miRNAs was finally examined in patient-matched laser-dissected primary tumors and lymph node metastases. Unsupervised clustering analysis largely separated primary tumors from lymph node metastases (Fig. 7A). A general reduced expression, including miR23b expression, was observed in lymph node metastases compared with primary tumors (Fig. 7A and B, box plots of selected miRNAs; of note, miR921 was not included in the assay platform version used here). Next, we performed GSEA of transcriptome profiles from 10 primary tumors and 12 lymph node metastases. A significant enrichment (FDR < 0.25 as defined by GSEA) of transcripts with target sites for exocytosis miR23b, miR224, miR144*, and miR143 was observed in the metastases. The data indicate a selective pressure for reduced expression of these tumor-suppressor miRNAs accompanied by increased expression of their putative targets during metastatic colonization.

Discussion

Three major findings are presented in this study. First, the intracellular level and activity of miR23b with tumor-suppressor function was influenced by exocytosis. Second, RAB27A and RAB27B were identified as regulators of exosomal miRNA secretion, of which high RAB27B expression correlated to poor prognosis of bladder cancer. Third, metastatic colonization *in vivo* was accompanied by loss of miRNAs, which were also identified as highly exocytosed from cultivated cells with a metastatic capacity. Our study highlights a possible intrinsic advantage for cancer cells to exit superfluous tumor-suppressor miRNAs via exosomes, a process that may support the metastatic cascade (modeled in Fig. 7C).

RAB27A and/or -B have been found previously to regulate secretion of secretory granules, exosomes, and soluble proteins (9, 32, 37). Functional redundancy has been reported in some model systems (38), whereas nonredundancy in others (9, 39). We observed comparable (and nonadditive) inhibition of exosome secretion, miR23b/miR921 exocytosis, and cellular invasion upon RAB27A and -B knockdown. This may suggest functions along the same pathway in our model system. Urothelial cells predominantly express RAB27B over RAB27A (32, 34). In accordance, we found little expression of

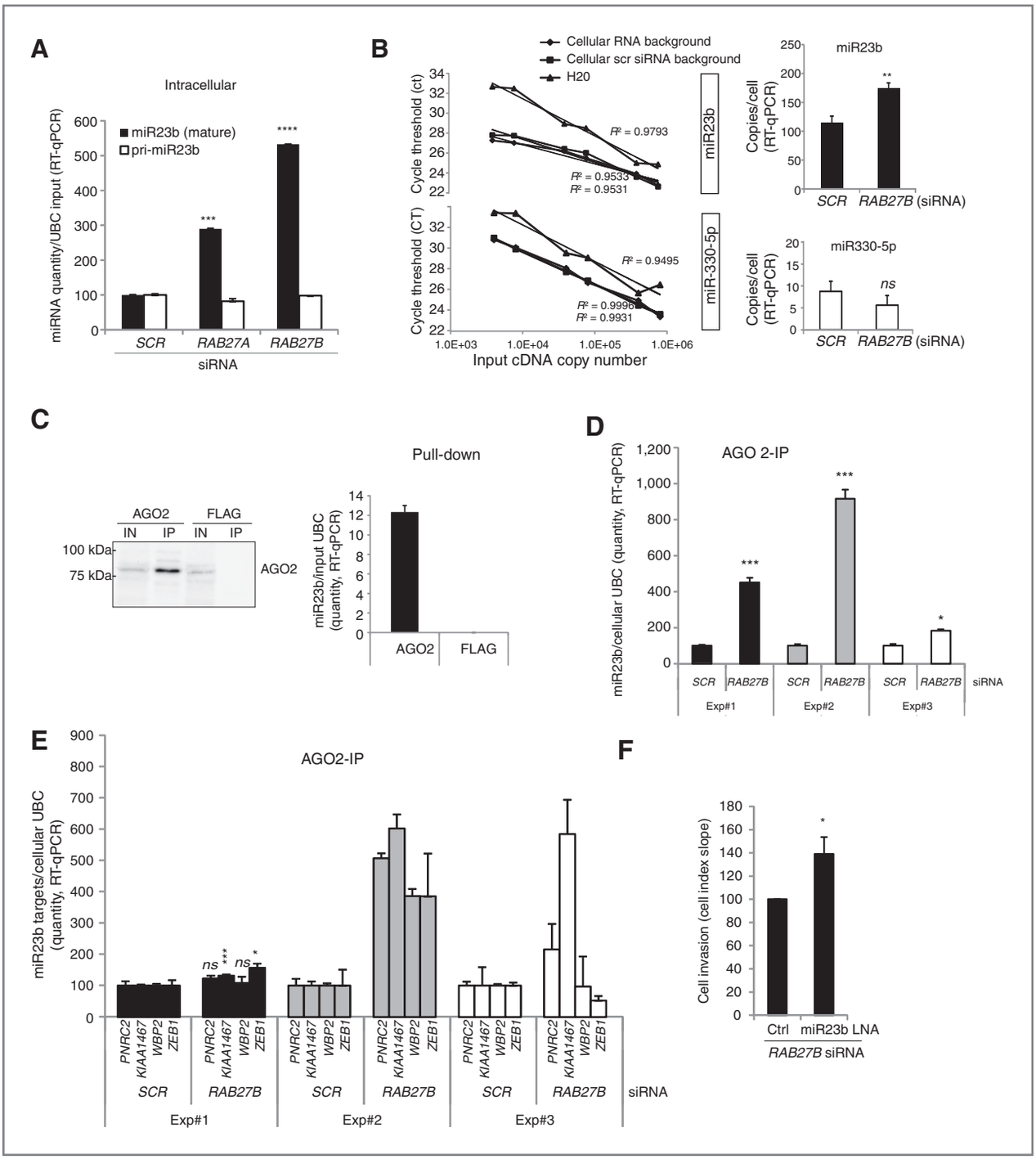

Figure 6. A, quantity of miR23b (mature) and primary miR23b (pri-miR23b) in FL3 cells 5 days after siRNA transfection. B, left, standard curves for miRNA copy assessment. Right, the intracellular exact copies of miR23b and -330-5p 5 days after transfection, calculated from the standard curves. C, immunoprecipitation (IP) using AGO2- or negative control (FLAG) antibody–coupled beads was performed on FL3 cell lysates. D, quantity of miR23b associated with AGO2 in three independent experiments of FL3 cells, 5 days after siRNA-transfection. E, in parallel, quantity of putative miR23b targets (PNRC2, KIAA1467, WBP2, and ZEB1) associated with AGO2. F, cellular invasion of FL3 cells 48 hours after transfection of siRNA ± LNA. Columns in A–C, averages of triplicate measurements; bars, SD. Data are representative of three triplicate experiments. Lines in B, averages of triplicates; bars, SD. Columns D and E, three independent experiments conducted in triplicates; bars, SD. Columns in F, averages of two experiments, each conducted in triplicates. ns, not significant; *, $P < 0.05$; **, $P < 0.01$; ***, $P < 0.001$.

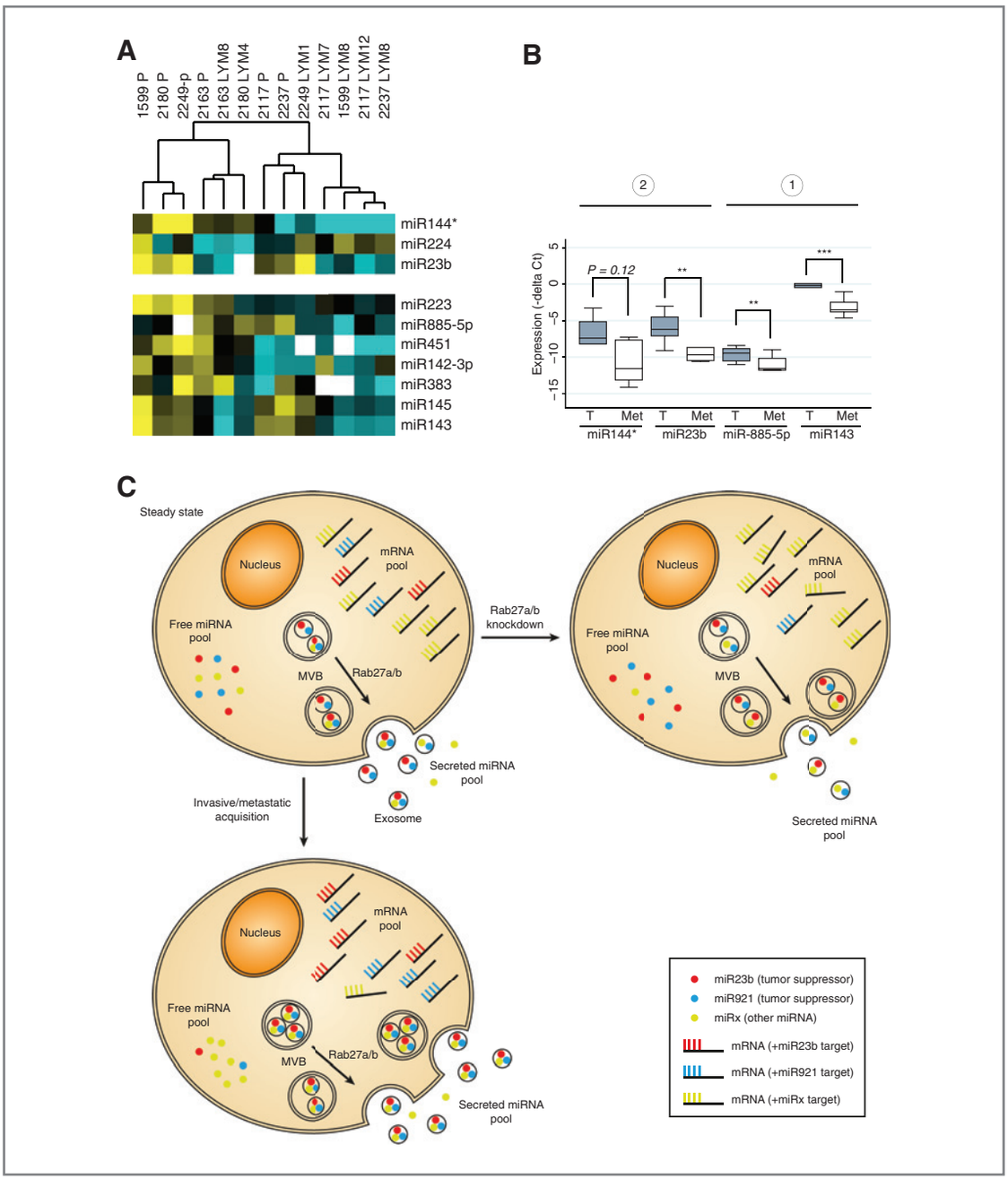

Figure 7. A, heatmap of unsupervised clustering analysis of exosome-miRNA expression in laser-dissected primary tumors and matched lymph node metastases (yellow, high expression values, low ΔC_t; blue, low expression values, high ΔC_t; white, absent values). B, box plots of the median expression of indicated miRNAs. C, proposed model of the regulatory circuit of intracellular and exocytosed miRNAs and mRNAs. The intracellular levels of mRNAs are regulated by miRNAs that bind targets leading to mRNA degradation. A subset of miRNAs is incorporated into intraluminal vesicles and cannot bind their mRNA targets, leading to increased cellular levels of target transcripts. Upon RAB27A/B knockdown, reduced exocytosis of specific miRNAs is observed (e.g., miR23b and miR921). This shifts the distribution of intracellular free miRNAs and increases degradation of their specific mRNA targets. Upon acquisition of a metastatic cellular state, increased relative secretion of miR23b and miR921 is observed. This may lead to reduced degradation of putative mRNA targets and, hence, increased cellular expression levels of these. Boxes in B, median expression; bars, SD. **, $P < 0.01$; ***, $P < 0.001$.

RAB27A in bladder cancer tumor cores. Previously, high RAB27B expression has been associated with presence of lymph node metastases among ER-positive breast cancer patients (40). In analogy, high RAB27B expression correlated with poor prognosis of bladder cancer. Whether this is mainly ascribed to increased RAB27B-dependent vesiculation or other identified RAB27B-mediated transcriptomic changes cannot be explicitly ascertained.

We identified a novel pathway for RAB27A/B-dependent cellular export of miRNAs. The majority of miR23b and miR921 was associated with 100,000 $\times g$ pelleted material, suggesting predominant exosome association rather than a soluble released form. We cannot entirely exclude that a fraction of 100,000 $\times g$-associated miR23b may be soluble and potentially contribute to the route of cellular disposal. miR23b was still secreted via the 100,000 $\times$ g fraction after RAB27A knockdown, which was not the case upon RAB27B knockdown (after which the remaining miR23b was present in the soluble fraction). This may suggest that subpopulations of miRNA-containing exosomes exist, and/or that inhibition of one exit route may redirect miRNAs destined for exocytosis to other secretory routes.

What could be the mechanism by which tumor-suppressor miRNAs are sorted into exosomes? Our data indicate that exocytosed miRNAs, in general, are decoupled from their repressive activity based on absence of miRISC proteins and depletion of their target transcripts in exosomes. It does not appear to be a passive consequence of increased MVB formation, as the MVB volume was only marginally increased in the metastatic cells. The cargo enclosure may be specified by tethering proteins that recruit excessive miRNAs. One study has identified miRNA sequence motifs and sumyolation status of hnRNPA2B1 to direct the sorting (20). We have identified several RNA-binding proteins of elevated abundance in exosomes from metastatic FL3 and SLT4 cells versus nonmetastatic T24 cells (e.g., hnRNPA3, -U, M, C1/C2; ref. 23), which could sequester specific miRNAs in metastatic cells. miRNAs may also be sorted into exosomes following 3′tail modifications (M. Pegtel and D. Koppers-Lalic, personal communication), of which some have been implicated in miRNA turnover (41). miRNAs are generally long-lived (average ~5 days, 10× fold that of mRNAs; ref. 42). It is, therefore, plausible that cellular export serves an auxiliary route to efficient elimination of undesired miRNAs. In line with this, selective exosomal disposal of miR150 was recently proposed as a rapid means to regulate gene expression during lymphocyte activation (43). Thus, a balance of "intracellular active" versus "exocytosis inactive" miRNAs is likely influencing the transcriptome as a whole.

The main focus of this study was the exocytic trafficking and function of miR23b. It reduced invasion (in FL3), resistance to anoikis, and *in vivo* angiogenesis and lung colonization in line with previous reports of miR23b being a pleiotropic metastasis suppressor (29). miR921 also showed remarkable metastatic-cell–specific and RAB27A/B-dependent exocytosis, but stable miR921 cell lines could unfortunately not be obtained. Overexpression of miR23b surprisingly inhibited invasion of FL3 cells and stimulated invasion of T24 cells, although target transcripts were downregulated in both cell lines. Variable secondary miRNA effects due to cellular context have previously been described (36), which could explain the overall opposite transcriptional changes and phenotype observed. miR23b displayed several metastasis-suppressive effects most prominent in the metastatic cell line (FL3), from which it was more highly exported.

Previous studies have documented reduced expression of miR23b, miR224, and miR921 in bladder- and prostate cancer (44–46), and reduced miR143/145 upon bladder cancer lymph node metastasis (47). We confirmed this latter finding and observed reduced expression of other identified exocytosis miRNAs accompanied by significant upregulation of their putative target transcripts in the metastases. The mechanism behind reduced expression is difficult to prove *in vivo*. Tumor-suppressor miRNAs are commonly lost due to epigenetic silencing, acquired mutations, or alterations in effector/repressor expression balance. We identified no or little evidence of miRNA gene mutations (Supplementary Fig. S4I; ref. 33) or epigenetic silencing of exocytosis miRNAs miR144, miR451, miR143, and miR145 in the TCGA bladder cancer dataset (Supplementary Fig. S4J). For miR23b, a modest correlation was observed, indicating epigenetic silencing as a likely contributing factor, but not in all cases. We did not attempt to mechanistically address miRNA vesiculation *in vivo*, which may be a limitation to the study. However such analysis is not trivial as circulating miRNAs originate from a range of cell types (and possibly from both primary tumor and metastases) and under influence of normal physiologic processes.

Our work may suggest a novel role for exosome release as a route to cellular disposal of miRNAs with the consequence to dampen intracellular effects on target transcripts. In this case, an intrinsic selective pressure for disposal of superfluous miR23b, which in turn may contribute to the transcriptomic changes associated with a cellular metastatic state. The model does not argue against exosomes as conveyors of cell-to-cell communication, but rather suggests the existence of a duality. On one side, exosome release may limit abundance of specific intracellular content and on the other side may affect other cells when the vesicular content is transferred.

Disclosure of Potential Conflicts of Interest

No potential conflicts of interest were disclosed.

Authors' Contributions

Conception and design: M.S. Ostenfeld, M.H. Rasmussen, T.F. Ørntoft
Development of methodology: M.S. Ostenfeld, D.K. Jeppesen, A.T. Boysen, B. Primdal-Bengtson, D. Theodorescu, K.A. Howard, L. Dyrskjøt
Acquisition of data (provided animals, acquired and managed patients, provided facilities, etc.): M.S. Ostenfeld, A.T. Boysen, B. Primdal-Bengtson, A. Hendrix, F. Dagnaes-Hansen, M.H. Rasmussen, K.H. Bui, N. Fristrup, E.I. Christensen, I. Nordentoft, J.P. Morth, J.B. Jensen, M. Borre, L. Dyrskjøt, T.F. Ørntoft
Analysis and interpretation of data (e.g., statistical analysis, biostatistics, computational analysis): M.S. Ostenfeld, J.R. Laurberg, A.T. Boysen, A. Hendrix, P. Lamy, N. Fristrup, E.I. Christensen, I. Nordentoft, J.S. Pedersen, L. Dyrskjøt
Writing, review, and/or revision of the manuscript: M.S. Ostenfeld, B. Primdal-Bengtson, A. Hendrix, P. Lamy, M.H. Rasmussen, E.I. Christensen, I. Nordentoft, J.B. Jensen, M. Beck, M. Borre, K.A. Howard, L. Dyrskjøt, T.F. Ørntoft
Administrative, technical, or material support (i.e., reporting or organizing data, constructing databases): M.S. Ostenfeld, A.T. Boysen, B. Primdal-Bengtson, M. Borre, L. Dyrskjøt
Study supervision: M.S. Ostenfeld, M. Beck
Other (experimental work): J.B. Bramsen

Acknowledgments

The authors thank Kasper Thorsen and Thomas Reinert for fruitful technical discussions and Susanne Bruun, Margaret Gellett, and Martin Rasmussen (Department of Clinical Pathology, Odense University Hospital) for technical assistance.

Grant Support

This work was supported by the Novo Nordisk Foundation, Toyota Foundation, Carlsberg Foundation, John and Birthe Meyer Foundation, Danish Research Council for Natural Sciences, Lundbeck Foundation, The Danish Cancer Biobank, Danish Cancer Society, and the European Community's FP7/2007-2011 (grant no. 201663).

The costs of publication of this article were defrayed in part by the payment of page charges. This article must therefore be hereby marked *advertisement* in accordance with 18 U.S.C. Section 1734 solely to indicate this fact.

Received December 11, 2013; revised July 10, 2014; accepted July 23, 2014; published OnlineFirst September 26, 2014.

References

1. Sternberg CN, Bellmunt J, Sonpavde G, Siefker-Radtke AO, Stadler WM, Bajorin DF, et al. ICUD-EAU International Consultation on Bladder Cancer 2012: chemotherapy for urothelial carcinoma-neoadjuvant and adjuvant settings. Eur Urol 2013;63:58–66.
2. Smith SC, Nicholson B, Nitz M, Frierson HF Jr, Smolkin M, Hampton G, et al. Profiling bladder cancer organ site-specific metastasis identifies LAMC2 as a novel biomarker of hematogenous dissemination. Am J Pathol 2009;174:371–9.
3. Overdevest JB, Thomas S, Kristiansen G, Hansel DE, Smith SC, Theodorescu D. CD24 offers a therapeutic target for control of bladder cancer metastasis based on a requirement for lung colonization. Cancer Res 2011;71:3802–11.
4. Gildea JJ, Seraj MJ, Oxford G, Harding MA, Hampton GM, Moskaluk CA, et al. RhoGDI2 is an invasion and metastasis suppressor gene in human cancer. Cancer Res 2002;62:6418–23.
5. Poste G, Nicolson GL. Arrest and metastasis of blood-borne tumor cells are modified by fusion of plasma membrane vesicles from highly metastatic cells. Proc Natl Acad Sci U S A 1980;77:399–403.
6. Hood JL, San RS, Wickline SA. Exosomes released by melanoma cells prepare sentinel lymph nodes for tumor metastasis. Cancer Res 2011;71:3792–801.
7. Peinado H, Aleckovic M, Lavotshkin S, Matei I, Costa-Silva B, Moreno-Bueno G, et al. Melanoma exosomes educate bone marrow progenitor cells toward a pro-metastatic phenotype through MET. Nat Med 2012;18:883–91.
8. Thery C, Zitvogel L, Amigorena S. Exosomes: composition, biogenesis and function. Nat Rev Immunol 2002;2:569–79.
9. Ostrowski M, Carmo NB, Krumeich S, Fanget I, Raposo G, Savina A, et al. Rab27a and Rab27b control different steps of the exosome secretion pathway. Nat Cell Biol 2010;12:19–30; sup pp 1–13.
10. Kosaka N, Iguchi H, Yoshioka Y, Takeshita F, Matsuki Y, Ochiya T. Secretory mechanisms and intercellular transfer of microRNAs in living cells. J Biol Chem 2010;285:17442–52.
11. Trajkovic K, Hsu C, Chiantia S, Rajendran L, Wenzel D, Wieland F, et al. Ceramide triggers budding of exosome vesicles into multivesicular endosomes. Science 2008;319:1244–7.
12. Johnstone RM, Adam M, Hammond JR, Orr L, Turbide C. Vesicle formation during reticulocyte maturation. Association of plasma membrane activities with released vesicles (exosomes). J Biol Chem 1987;262:9412–20.
13. Chairoungdua A, Smith DL, Pochard P, Hull M, Caplan MJ. Exosome release of beta-catenin: a novel mechanism that antagonizes Wnt signaling. J Cell Biol 2010;190:1079–91.
14. Verweij FJ, van Eijndhoven MA, Hopmans ES, Vendrig T, Wurdinger T, Cahir-McFarland E, et al. LMP1 association with CD63 in endosomes and secretion via exosomes limits constitutive NF-kappaB activation. EMBO J 2011;30:2115–29.
15. Putz U, Howitt J, Doan A, Goh CP, Low LH, Silke J, et al. The tumor suppressor PTEN is exported in exosomes and has phosphatase activity in recipient cells. Sci Signal 2012;5:ra70.
16. Valadi H, Ekstrom K, Bossios A, Sjostrand M, Lee JJ, Lotvall JO. Exosome-mediated transfer of mRNAs and microRNAs is a novel mechanism of genetic exchange between cells. Nat Cell Biol 2007;9:654–9.
17. Mittelbrunn M, Gutierrez-Vazquez C, Villarroya-Beltri C, Gonzalez S, Sanchez-Cabo F, Gonzalez MA, et al. Unidirectional transfer of microRNA-loaded exosomes from T cells to antigen-presenting cells. Nat Commun 2011;2:282.
18. Al-Nedawi K, Meehan B, Micallef J, Lhotak V, May L, Guha A, et al. Intercellular transfer of the oncogenic receptor EGFRvIII by microvesicles derived from tumour cells. Nat Cell Biol 2008;10:619–24.
19. Pigati L, Yaddanapudi SC, Iyengar R, Kim DJ, Hearn SA, Danforth D, et al. Selective release of microRNA species from normal and malignant mammary epithelial cells. PLoS ONE 2010;5:e13515.
20. Villarroya-Beltri C, Gutierrez-Vazquez C, Sanchez-Cabo F, Perez-Hernandez D, Vazquez J, Martin-Cofreces N, et al. Sumoylated hnRNPA2B1 controls the sorting of miRNAs into exosomes through binding to specific motifs. Nat Commun 2013;4:2980.
21. Batagov AO, Kurochkin IV. Exosomes secreted by human cells transport largely mRNA fragments that are enriched in the 3′-untranslated regions. Biol Direct 2013;8:12.
22. Le XF, Merchant O, Bast RC, Calin GA. The roles of MicroRNAs in the cancer invasion-metastasis cascade. Cancer Microenviron 2010;3:137–47.
23. Jeppesen DK, Nawrocki A, Jensen SG, Thorsen K, Whitehead B, Howard KA, et al. Quantitative proteomics of fractionated membrane and lumen exosome proteins from isogenic metastatic and nonmetastatic bladder cancer cells reveal differential expression of EMT factors. Proteomics 2014;14:699–712.
24. Ostenfeld MS, Hoyer-Hansen M, Bastholm L, Fehrenbacher N, Olsen OD, Groth-Pedersen L, et al. Anti-cancer agent siramesine is a lysosomotropic detergent that induces cytoprotective autophagosome accumulation. Autophagy 2008;4:487–99.
25. Jensen SG, Lamy P, Rasmussen MH, Ostenfeld MS, Dyrskjot L, Orntoft TF, et al. Evaluation of two commercial global miRNA expression profiling platforms for detection of less abundant miRNAs. BMC Genomics 2011;12:435.
26. Dyrskjøt L, Ostenfeld MS, Bramsen JB, Silahtaroglu AN, Lamy P, Ramanathan R, et al. Genomic profiling of microRNAs in bladder cancer: miR-129 is associated with poor outcome and promotes cell death *in vitro*. Cancer Res 2009;69:4851–60.
27. Ostenfeld MS, Bramsen JB, Lamy P, Villadsen SB, Fristrup N, Sorensen KD, et al. miR-145 induces caspase-dependent and -independent cell death in urothelial cancer cell lines with targeting of an expression signature present in Ta bladder tumors. Oncogene 2010;29:1073–84.
28. Kosaka N, Iguchi H, Hagiwara K, Yoshioka Y, Takeshita F, Ochiya T. Neutral sphingomyelinase 2 (nSMase2)-dependent exosomal transfer of angiogenic microRNAs regulate cancer cell metastasis. J Biol Chem 2013;288:10849–59.
29. Zhang H, Hao Y, Yang J, Zhou Y, Li J, Yin S, et al. Genome-wide functional screening of miR-23b as a pleiotropic modulator suppressing cancer metastasis. Nat Commun 2011;2:554.
30. Nicholson BE, Frierson HF, Conaway MR, Seraj JM, Harding MA, Hampton GM, et al. Profiling the evolution of human metastatic bladder cancer. Cancer Res 2004;64:7813–21.
31. Gildea JJ, Golden WL, Harding MA, Theodorescu D. Genetic and phenotypic changes associated with the acquisition of tumorigenicity in human bladder cancer. Genes Chromosomes Cancer 2000;27:252–63.
32. Bobrie A, Krumeich S, Reyal F, Recchi C, Moita LF, Seabra MC, et al. Rab27a supports exosome-dependent and -independent mechanisms that modify the tumor microenvironment and can promote tumor progression. Cancer Res 2012;72:4920–30.
33. Nordentoft I, Lamy P, Birkenkamp-Demtroder K, Shumansky K, Vang S, Hornshoj H, et al. Mutational context and diverse clonal development in early and late bladder cancer. Cell Rep 2014;7:1649–63.
34. Chen Y, Guo X, Deng FM, Liang FX, Sun W, Ren M, et al. Rab27b is associated with fusiform vesicles and may be involved in targeting uroplakins to urothelial apical membranes. Proc Natl Acad Sci U S A 2003;100:14012–7.

35. Hammond SM, Boettcher S, Caudy AA, Kobayashi R, Hannon GJ. Argonaute2, a link between genetic and biochemical analyses of RNAi. Science 2001;293:1146–50.
36. Nam JW, Rissland OS, Koppstein D, Abreu-Goodger C, Jan CH, Agarwal V, et al. Global analyses of the effect of different cellular contexts on microRNA targeting. Mol Cell 2014;53:1031–43.
37. Mizuno K, Tolmachova T, Ushakov DS, Romao M, Abrink M, Ferenczi MA, et al. Rab27b regulates mast cell granule dynamics and secretion. Traffic 2007;8:883–92.
38. Barral DC, Ramalho JS, Anders R, Hume AN, Knapton HJ, Tolmachova T, et al. Functional redundancy of Rab27 proteins and the pathogenesis of Griscelli syndrome. J Clin Invest 2002;110:247–57.
39. Singh RK, Mizuno K, Wasmeier C, Wavre-Shapton ST, Recchi C, Catz SD, et al. Distinct and opposing roles for Rab27a/Mlph/MyoVa and Rab27b/Munc13-4 in mast cell secretion. FEBS J 2013;280:892–903.
40. Hendrix A, Maynard D, Pauwels P, Braems G, Denys H, Van den Broecke R, et al. Effect of the secretory small GTPase Rab27B on breast cancer growth, invasion, and metastasis. J Natl Cancer Inst 2010;102:866–80.
41. Jones MR, Quinton LJ, Blahna MT, Neilson JR, Fu S, Ivanov AR, et al. Zcchc11-dependent uridylation of microRNA directs cytokine expression. Nat Cell Biol 2009;11:1157–63.
42. Gantier MP, McCoy CE, Rusinova I, Saulep D, Wang D, Xu D, et al. Analysis of microRNA turnover in mammalian cells following Dicer1 ablation. Nucleic Acids Res 2011;39:5692–703.
43. de Candia P, Torri A, Gorletta T, Fedeli M, Bulgheroni E, Cheroni C, et al. Intracellular modulation, extracellular disposal and serum increase of MiR-150 mark lymphocyte activation. PLoS ONE 2013;8:e75348.
44. Majid S, Dar AA, Saini S, Deng G, Chang I, Greene K, et al. MicroRNA-23b functions as a tumor suppressor by regulating Zeb1 in bladder cancer. PLoS ONE 2013;8:e67686.
45. Kristensen H, Haldrup C, Strand S, Mundbjerg K, Mortensen MM, Thorsen K, et al. Hypermethylation of the GABRE∼miR-452∼miR-224 promoter in prostate cancer predicts biochemical recurrence after radical prostatectomy. Clin Cancer Res 2014;20:2169–81.
46. Pignot G, Cizeron-Clairac G, Vacher S, Susini A, Tozlu S, Vieillefond A, et al. microRNA expression profile in a large series of bladder tumors: identification of a 3-miRNA signature associated with aggressiveness of muscle-invasive bladder cancer. Int J Cancer 2013;132:2479–91.
47. Baffa R, Fassan M, Volinia S, O'Hara B, Liu CG, Palazzo JP, et al. MicroRNA expression profiling of human metastatic cancers identifies cancer gene targets. J Pathol 2009;219:214–21.